

## Ground state of the Sn/Ge(111)- $3\times 3$ surface and its electron-beam-induced disordering

Tetsuroh Shirasawa,<sup>1,\*</sup> Hiroshi Tochihara,<sup>2</sup> Kimitaka Kubo,<sup>1</sup> Wolfgang Voegeli,<sup>1</sup> and Toshio Takahashi<sup>1</sup>

<sup>1</sup>*Institute for Solid State Physics, University of Tokyo, Chiba 277-8581, Japan*

<sup>2</sup>*Department of Molecular and Material Sciences, Kyushu University, Fukuoka 816-8580, Japan*

(Received 25 January 2010; published 25 February 2010)

Low-energy electron diffraction (LEED) studies at 14 K revealed that the ground state of the Sn/Ge(111)- $3\times 3$  surface is the so-called one-Sn-up and two-Sn-down (1U2D) structure. The electron beam in the LEED observation was found to disorder the 1U2D structure below  $\sim 40$  K. Cross sections for the structural change suggest that an interband transition between Sn-derived surface state bands becomes the trigger for the structural change. A mechanism of the excitation-induced structural change activated below  $\sim 40$  K is discussed.

DOI: [10.1103/PhysRevB.81.081409](https://doi.org/10.1103/PhysRevB.81.081409)

PACS number(s): 61.05.jh, 61.80.Fe

Ground states of low-dimensional materials are often characterized by electron-lattice interaction and electron-electron interaction since the effect of these interactions becomes more important in reduced dimensions. A remarkable example of such a two-dimensional system is the  $(\sqrt{3}\times\sqrt{3})R30^\circ$  triangular array of Sn adatoms on the Ge(111) surface. The dangling bond of the Sn adatom produces a narrow metallic surface state band within the substrate's band gap. The ideal two-dimensional metallic phase is stabilized by introducing a  $3\times 3$  periodic vertical distortion of the Sn atoms,<sup>1</sup> where one Sn atom in the unit cell is located at a position higher than the other two Sn atoms [see Fig. 2(b)].<sup>2-5</sup> The so-called 1-up and 2-down (1U2D) distortion is correlated with the electron transfer from the down Sn atoms to the up Sn atom,<sup>6,7</sup> achieving a net energy gain of the system. Above  $\sim 200$  K, the 1U2D long-range order is destroyed by thermally induced vertical fluctuations of the Sn atoms, resulting in the apparent  $(\sqrt{3}\times\sqrt{3})R30^\circ$  periodicity.<sup>8-10</sup>

The  $3\times 3$ -1U2D low-temperature phase had been believed to be the ground state of the Sn/Ge(111) surface. However, very recently, it was reported that the  $3\times 3$  structure changes into a new  $(\sqrt{3}\times\sqrt{3})R30^\circ$  structure below 30 K with gap opening of a metallic band, on the basis of low-energy electron diffraction (LEED), scanning tunneling microscopy (STM), and photoemission spectroscopy (PES) experiments.<sup>11</sup> The newly found ground state was attributed to a Mott-Hubbard insulator due to the electron correlation in the narrow metallic band.<sup>11,12</sup>

However, the insulating ground state has been questioned by subsequent STM and spectroscopy (STS) studies.<sup>13,14</sup> Colonna *et al.* observed a metallic  $3\times 3$  structure down to 2.5 K by STS, and hence the metal-insulator transition was denied. They have suggested that an STM tip-surface interaction becomes active below  $\sim 20$  K to excite dynamical vertical fluctuations of the Sn atoms, leading to the apparent  $(\sqrt{3}\times\sqrt{3})R30^\circ$  periodicity in STM images.<sup>13</sup> Morikawa *et al.* also observed a metallic  $3\times 3$  structure down to 4 K by STS, but they have ruled out the tip effect. They have observed that the local density of states of a surface state changes below  $\sim 20$  K and proposed that the surface settles into a new  $3\times 3$  structure modified from the  $3\times 3$  structure stable above 20 K.<sup>14</sup> Consensus is not reached on the nature of the ground state.<sup>15</sup>

In this Rapid Communication, we report on the structural

nature of the Sn/Ge(111) surface studied by LEED experiments. The  $3\times 3$ -1U2D structure is confirmed as the ground state even at 14 K. Interestingly, the electron beam (EB) in the LEED observation is found to induce disorder in the  $3\times 3$  domain below  $\sim 40$  K. The  $3\times 3$ - $(\sqrt{3}\times\sqrt{3})R30^\circ$  transition observed in Ref. 11 stems from the probe effect. A mechanism that can explain the EB-induced structural change activated below  $\sim 40$  K is proposed.

A commercial Ge(111) wafer (*p* type, 0.1  $\Omega$  cm) was used as the substrate. The Sn/Ge(111) surface was prepared with a standard procedure.<sup>10</sup> One-third monolayer of Sn was deposited to maximize the intensity of the  $(\sqrt{3}\times\sqrt{3})R30^\circ$  LEED spots at room temperature. The possible error of the coverage estimation was 5%. The intensity distribution of the LEED pattern was acquired with a charge coupled device (CCD) camera with an acquisition time of  $\sim 1.9$  s. Sample temperatures were monitored with a calibrated thermocouple. Current densities of the EB were measured with a Faraday cup within 5% error. The vacuum pressure during LEED measurements was below  $5\times 10^{-9}$  Pa. The surface structural change was investigated by the spot profile analysis: the integer order spots and the one-third order spots specific to the  $(\sqrt{3}\times\sqrt{3})R30^\circ$  periodicity (hereafter  $\sqrt{3}\times\sqrt{3}$  spots) were fitted with a Gaussian, and the one-third order spots specific to the  $3\times 3$  periodicity (hereafter  $3\times 3$  spots) with a Lorentzian convoluted with an instrumental response function.<sup>16,17</sup>

First, we investigated the ground state of the Sn/Ge(111) surface. We cooled the Sn/Ge(111) surface from room temperature down to 14 K with a cooling rate of  $\sim 0.1$  K/s, while observing the LEED pattern. Figure 1(a) shows the temperature dependence of the LEED spots, where (1 0), (4/3 1/3), and (0 1/3) spots correspond to the integer order,  $\sqrt{3}\times\sqrt{3}$ , and  $3\times 3$  spots, respectively. The upper panel shows the peak height of the spot profile, and the lower panel shows the correlation length of the  $3\times 3$  structure obtained from the inverse of the Lorentzian width of the  $3\times 3$  spot. At room temperature, LEED exhibits the  $(\sqrt{3}\times\sqrt{3})R30^\circ$  pattern. With decreasing sample temperature, diffuse  $3\times 3$  spots appear and change into bright, sharp spots below  $\sim 150$  K. This  $(\sqrt{3}\times\sqrt{3})R30^\circ$ - $3\times 3$  phase transition is caused by the freezing of the thermally activated vertical fluctuations of the Sn atoms.<sup>4,5</sup> The atomic arrangement of the  $3\times 3$  phase at 80 K was determined by the LEED *I-V* (spot intensity versus incident energy) analysis. Theoretical *I-V* spectra were cal-

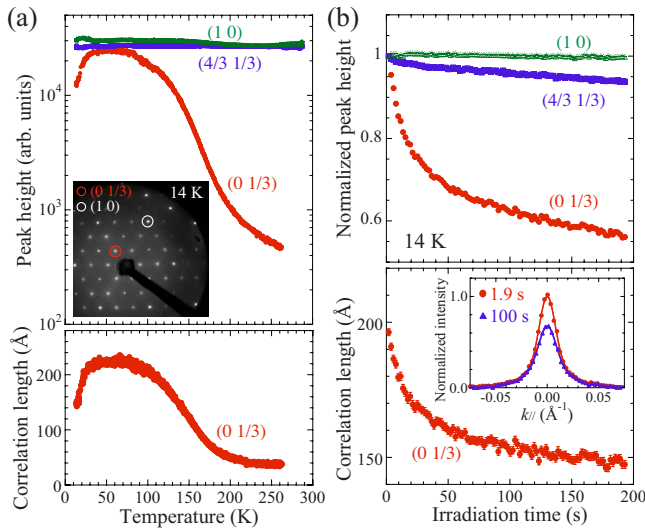


FIG. 1. (Color online) (a) Temperature dependence of LEED spot profiles. Upper panel shows peak height, where the Debye-Waller factor was subtracted; lower panel exhibits correlation length of the  $3 \times 3$  structure [inverse of the Lorentzian width of the (0 1/3) spot]. Inset in the upper panel is the  $3 \times 3$  LEED pattern observed at 14 K. (b) Change in the LEED spot profiles as a function of EB irradiation time at 14 K. Upper panel shows normalized peak height; lower panel shows the correlation length of the  $3 \times 3$  structure. Inset in the lower panel shows profiles of the (0 1/3) spot measured at EB irradiation times of 1.9 and 100 s at 14 K, where solid lines are the resolution-convoluted Lorentzians.

culated on the basis of a dynamical diffraction theory by using the Barbieri–Van Hove symmetrized automated tensor LEED package.<sup>18</sup> 4650 data points for 29 symmetrically inequivalent spots were used to optimize the 27 structural parameters shown in Fig. 2(b). The 1U2D structure shown in Fig. 2(b) was confirmed with good reliability (the Pendry  $R$  factor<sup>19</sup> is 0.17). The  $I$ - $V$  spectra measured at 80 K and calculated ones for the best-fit structure agree very well [see five curves in Fig. 2(a); other 24 curves also show good agreement]. The height difference between the up and down Sn atoms is  $0.38 \pm 0.09$  Å. The heights of the two down Sn atoms are the same within the error range of 0.05 Å. These results agree with previous reports.<sup>2,3</sup> The tiny height difference between the down Sn atoms recently suggested<sup>20</sup> might be within the error range of 0.05 Å.

Upon further cooling, the peak height and the correlation length of the  $3 \times 3$  spot decreased simultaneously below  $\sim 40$  K as seen in Fig. 1(a). This change indicates that the 1U2D domain size decreases below  $\sim 40$  K, in agreement with the disappearance of the  $3 \times 3$  structure below 30 K reported in Ref. 11. The reduction in the  $3 \times 3$  domain has been attributed to the structural change to a new  $(\sqrt{3} \times \sqrt{3})R30^\circ$  structure in Ref. 11 or a new  $3 \times 3$  structure in Ref. 14. To elucidate the structural change  $I$ - $V$  spectra were measured at 14 K. The  $I$ - $V$  spectra were taken after the cooling measurement in Fig. 1(a). The shape of the  $I$ - $V$  spectra at 14 K are identical to those at 80 K as seen in Fig. 3(a). The absence of new features denies the formation of new ordered structures at 14 K. Figure 1(a) shows that only the  $3 \times 3$  spots are weakened below  $\sim 40$  K, and the  $\sqrt{3} \times \sqrt{3}$  spots are

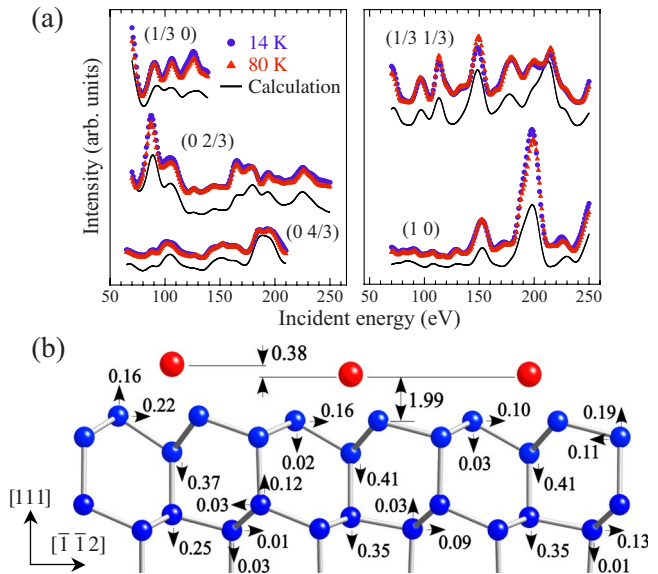


FIG. 2. (Color online) (a) Experimental  $I$ - $V$  spectra of LEED spots at 80 and 14 K and calculated ones for the  $3 \times 3$ -1U2D structure optimized by the LEED  $I$ - $V$  analysis at 80 K. Each  $I$ - $V$  spectrum is arbitrary weighted for comparison. (b) Cross-sectional view of the optimized  $3 \times 3$ -1U2D structure. Displacements of inequivalent Ge atoms relative to bulk positions in  $[111]$  and  $[\bar{1}\bar{1}2]$  directions are given in Å. Height difference between higher and lower Sn atoms is  $0.38 \pm 0.09$  Å. The error range of structural parameter was derived from variance of the Pendry  $R$ -factor (Ref. 19). The error range of every vertical position is below 0.06 Å. The error range of every lateral position is below 0.1 Å above the bottom Ge bilayer and below 0.15 Å at the bottom Ge bilayer.

almost unaffected. This suggests that the 1U2D height distribution of the Sn atoms is partially disordered below  $\sim 40$  K with the  $(\sqrt{3} \times \sqrt{3})R30^\circ$  lateral distribution preserved.

Interestingly, the disordering of the 1U2D structure is not due to an intrinsic structural transition as demonstrated below. We cooled the sample down to 14 K without the LEED observation, i.e., without the EB irradiation, and then started the LEED observation as a function of the irradiation time at 14 K. The condition of the EB was 90 eV and  $0.56 \mu\text{A}/\text{mm}^2$ , being the same as in the temperature dependence measurement in Fig. 1(a). Figure 1(b) shows changes in the LEED spots as a function of the irradiation time. At first the LEED pattern showed sharp  $3 \times 3$  spots, but they became weaker and broader after  $\sim 100$  s [see the inset in Fig. 1(b)]. The peak height of the  $3 \times 3$  spot (the upper panel) and the correlation length (the lower panel) decreased rapidly with the irradiation time, while the integer order and  $\sqrt{3} \times \sqrt{3}$  spots are almost unaffected. These changes coincide with those in the temperature dependence below  $\sim 40$  K [cf. Fig. 1(a)]. After the measurement we moved the sample to a nonirradiated area and restarted the same measurement. This gave the same result. These facts demonstrate that the disordering of the  $3 \times 3$ -1U2D height distribution below  $\sim 40$  K is caused by the EB irradiation. The intrinsic ground state is the  $3 \times 3$ -1U2D structure even at 14 K.

Figure 3(a) shows changes in the peak height of the  $3 \times 3$  spot as a function of the EB irradiation time, measured

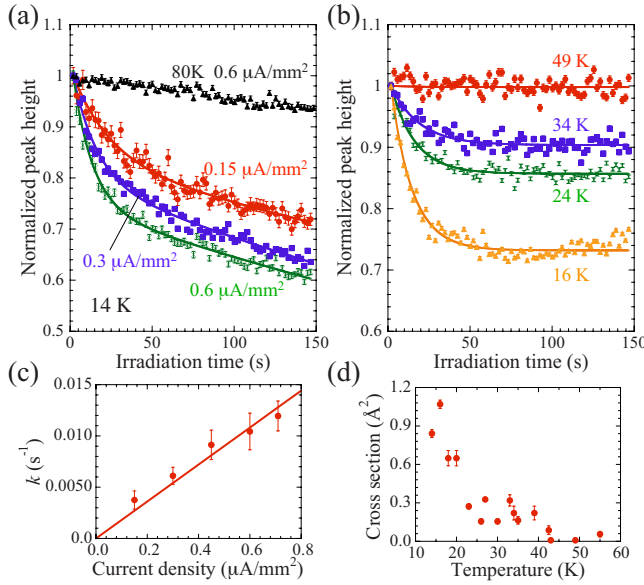


FIG. 3. (Color online) Current density dependence (a) and temperature dependence (b) of change in the peak height of (0 1/3) spot. Solid curves are the fitted curves. In (a) EB energy is 50 eV and temperature is 14 K. The peak height change measured at 80 K is also plotted in (a). In (b) EB energy is 50 eV and current density is 0.6  $\mu\text{A}/\text{mm}^2$ . (c) Current density dependence of the reduction rate  $k$  of the  $3 \times 3$  area. The solid line is a fitted linear line, where a condition  $k=0$  at the current density=0 is imposed. (d) Temperature dependence of the cross section for the structural change.

with three EB current densities at 14 K. These curves appear to have two components: an initial rapid decrease terminating before  $\sim 70$  s and a subsequent slow one. The slope of the initial rapid decrease becomes steeper with increasing the current density, indicating that it stems from the EB-induced disordering. On the other hand, the slope of the slow component is almost independent of the current density, indicating that this decrease is not caused by incoming electrons. Such current-independent slow decrease was also observed at 80 K [Fig. 3(a)], where the EB-induced rapid decay does not occur. A probable cause of the current-independent decrease is the surface degradation by the adsorption of residual gas at low temperatures. Such surface degradation during LEED measurement at low temperatures was also observed on the Si(001) clean surface.<sup>21</sup>

In order to evaluate the efficiency of the EB-induced structural change quantitatively, a curve-fitting analysis was conducted. We described the peak height at an irradiation time  $t$  as  $[F_{\text{EB}}(t)\exp(-ct)]^2$ .  $F_{\text{EB}}(t)$  is the absolute value of the scattering amplitude at the profile peak, and  $\exp(-ct)$  represents the constant decrease in the amplitude due to the adsorption with an attenuation constant  $c$  (typically 0.005  $\text{s}^{-1}$  at 14 K). We formulated the time variation in  $F_{\text{EB}}(t)$  as a rate equation

$$\frac{dF_{\text{EB}}(t)}{dt} = -kF_{\text{EB}}(t) + r[F_{\text{EB}}(0) - F_{\text{EB}}(t)], \quad (1)$$

where  $k$  is the rate constant for the reduction in the  $3 \times 3$  area. The  $3 \times 3$  spots weakened by the EB irradiation recover

by heating the sample up to  $\sim 50$  K. Thus, the second term in Eq. (1) was added to represent the thermal reordering of the disordered area with the rate constant  $r$  (typically 0.1  $\text{s}^{-1}$  at 39 K).  $F_{\text{EB}}(t)$  can be obtained as

$$F_{\text{EB}}(t) = \frac{F_{\text{EB}}(0)}{r+k} \{r+k \exp[-(r+k)t]\}. \quad (2)$$

The fitted curves reproduce the experimental ones very well as shown in Fig. 3(a). The current density dependence of  $k$  is shown in Fig. 3(c), where the average value of five measurements is plotted with the standard deviation (error bar) for each current density.  $k$  depends on the current density almost linearly, indicating that the structural change is induced by single electrons. We define the cross section for the structural change for an incident electron as  $\sigma = k/(N \times A_{\text{Sn}})$ , where  $N$  is the electron dose per area per second.  $A_{\text{Sn}}$  is the area fraction of the Sn layer, assumed to be 1/3 from the Sn coverage. The slope of the linear-fit line in Fig. 3(c) gives  $0.86 \pm 0.09 \text{ \AA}^2$  as the cross section for 50-eV electrons at 14 K [hereafter  $\sigma(14 \text{ K})$ ].

Such low-energy electrons can change surface structures through core-level excitations<sup>22</sup> or valence-band excitations.<sup>21,23</sup> Here we infer the electronic state relevant to the structural change by comparing the value of  $\sigma(14 \text{ K})$  to ionization cross sections calculated for an isolated Sn atom for a 50-eV electron.<sup>24</sup> The ionization cross section for the 4d level is smaller than the value of  $\sigma(14 \text{ K})$  by one order of magnitude, and hence the core-level excitation can be ruled out. On the other hand, the cross sections for the 5s and 5p levels are one order larger than the value of  $\sigma(14 \text{ K})$ .<sup>25</sup> Therefore, excitations of Sn-derived valence bands can be a reasonable candidate. In the Sn/Ge(111) surface, the 1U2D displacement splits the metallic surface state band into a semiconducting surface band highly localized on the “up” Sn atom (hereafter “up band”) and a quarter-filled band and an unoccupied band on the “down” Sn atoms (hereafter “down bands”), which leads to the charge transfer from the down Sn atoms to the up one.<sup>7</sup> Therefore, the charge transfer between the up and down Sn atoms should be correlated with the vertical motion of the Sn atoms. We thus suggest that the interband transitions from the up band to the down bands is the trigger for the vertical motion.

The EB effect depends on temperature significantly. The changes in the peak height of the  $3 \times 3$  spot at different temperatures are shown in Fig. 3(b), where the adsorption-induced factor,  $\exp(-2ct)$ , was subtracted. The intensity decrease is negligible at 49 K and becomes greater as the temperature is lowered. In Fig. 3(d), the temperature dependence of  $\sigma$  shows that the EB effect occurs below  $\sim 40$  K and increases significantly below  $\sim 20$  K. Colonna *et al.* also reported that the STM-tip-induced fluctuation of the Sn atoms becomes active below  $\sim 20$  K.<sup>13</sup> Therefore, a change in a property of the system below  $\sim 40$  K would lead to the structural instability against the external stimuli.

Such structural instability also occurs in the Si(001) clean surface, where the buckling orientation of the surface Si dimer can be changed by the EB or STM current only below  $\sim 50$  K.<sup>21,26</sup> A vibrational ladder climbing model explains the mechanism of the dimer flipping.<sup>21,27</sup> The ladder climb-

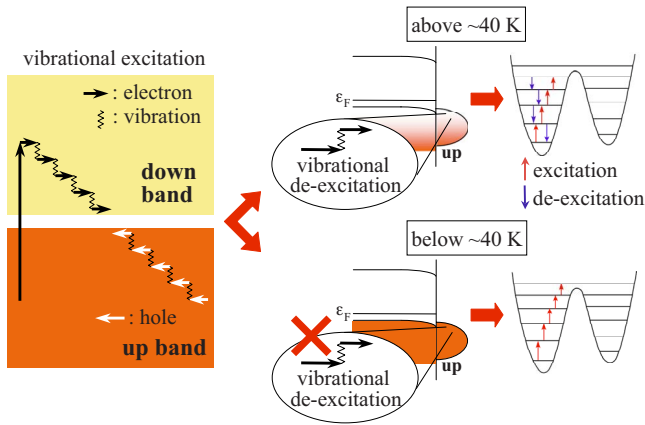


FIG. 4. (Color online) The proposed process of the excitation-induced motion of the Sn atom below 40 K. Left side: successive excitations of the vertical vibration of the Sn atoms through the decay of the interband excitation from the up band to down bands. Upper right: de-excitation of the vibration by the vibration-mediated electronic transition in the up band above 40 K. Lower right: suppression of the vibrational deexcitation below 40 K due to filling of the up band.

ing model depicted in Fig. 4 can also explain the excitation-induced Sn motion. In this model, filling of the semiconducting “up band” below 40 K leads to the structural instability. After the interband transition from the up band to the down band, the electronic excitation energy can be transferred to the lattice energy by creating a number of the vibrations associated with the vertical motion of the Sn atoms<sup>28</sup> due to the strong electron-lattice coupling (the left side in Fig. 4).

Above 40 K, the vibrations can be immediately absorbed by the vibration-mediated electronic transitions in the surface bands (the upper right in Fig. 4). With decreasing temperature, the thermally created hole population in the semiconducting up band is reduced. The filling of the up band leads to the decrease in the probability of the inner-band electronic transition in the up band. Thus, the vibrations created through the decay of the electronic excitation cannot be immediately absorbed by the inner-band electronic transition in the up band below 40 K, leading the Sn atoms into high vibrational states enough to overcome the potential barrier for switching their vertical positions (the lower right in Fig. 4).

In conclusion, the LEED studies revealed that the ground state of the Sn/Ge(111) surface is the  $3 \times 3$ -1U2D structure. The EB starts to disorder the 1U2D structure below  $\sim 40$  K. The interband transition from the up band to the down band is suggested to cause the vertical motion of the Sn atoms. The ladder climbing model, which explains the similar structural change in the Si(001) clean surface, can also explain the structural change in the Sn/Ge(111) surface. Similar excitation-induced structural change can likely occur as well on other semiconductor surfaces that have the relevant properties common to the two surfaces: a semiconducting surface band, energetically nearly degenerate structures, and their strong electron-lattice coupling.

The authors acknowledge the partial financial support of Grant-in Aid for Scientific Research (B) (Grant No. 19340083).

\*sirasawa@issp.u-tokyo.ac.jp

<sup>1</sup>J. M. Carpinelli *et al.*, *Nature* (London) **381**, 398 (1996).

<sup>2</sup>O. Bunk *et al.*, *Phys. Rev. Lett.* **83**, 2226 (1999).

<sup>3</sup>J. Zhang *et al.*, *Phys. Rev. B* **60**, 2860 (1999).

<sup>4</sup>L. Floreano *et al.*, *Phys. Rev. B* **64**, 075405 (2001).

<sup>5</sup>L. Petaccia *et al.*, *Phys. Rev. B* **64**, 193410 (2001).

<sup>6</sup>G. Ballabio *et al.*, *Phys. Rev. Lett.* **89**, 126803 (2002).

<sup>7</sup>J. Ortega, R. Pérez, and F. Flores, *J. Phys.: Condens. Matter* **14**, 5979 (2002).

<sup>8</sup>R. I. G. Uhrberg and T. Balasubramanian, *Phys. Rev. Lett.* **81**, 2108 (1998).

<sup>9</sup>J. Avila *et al.*, *Phys. Rev. Lett.* **82**, 442 (1999).

<sup>10</sup>F. Ronci *et al.*, *Phys. Rev. Lett.* **95**, 156101 (2005).

<sup>11</sup>R. Cortés *et al.*, *Phys. Rev. Lett.* **96**, 126103 (2006).

<sup>12</sup>G. Profeta and E. Tosatti, *Phys. Rev. Lett.* **98**, 086401 (2007).

<sup>13</sup>S. Colonna *et al.*, *Phys. Rev. Lett.* **101**, 186102 (2008).

<sup>14</sup>H. Morikawa, S. Jeong, and H. W. Yeom, *Phys. Rev. B* **78**, 245307 (2008).

<sup>15</sup>H. Morikawa and H. W. Yeom, *Phys. Rev. Lett.* **102**, 159601 (2009); S. Colonna *et al.*, *ibid.* **102**, 159602 (2009).

<sup>16</sup>L. D. Roelofs *et al.*, *Phys. Rev. Lett.* **46**, 1465 (1981).

<sup>17</sup>The typical  $3 \times 3$  domain size of 120–200 Å (Refs. 2 and 4) is comparable to the transfer width of the LEED apparatus of  $\sim 150$  Å. As the instrumental response function a Gaussian fitted to the integer-order spot was used (Ref. 16).

<sup>18</sup>M. A. Van Hove *et al.*, *Surf. Sci. Rep.* **19**, 191 (1993).

<sup>19</sup>J. B. Pendry, *J. Phys. C* **13**, 937 (1980).

<sup>20</sup>A. Tejeda *et al.*, *Phys. Rev. Lett.* **100**, 026103 (2008).

<sup>21</sup>T. Shirasawa, S. Mizuno, and H. Tochiara, *Phys. Rev. Lett.* **94**, 195502 (2005).

<sup>22</sup>O. Dulub *et al.*, *Science* **317**, 1052 (2007).

<sup>23</sup>K. Nakayama and J. H. Weaver, *Phys. Rev. Lett.* **82**, 980 (1999).

<sup>24</sup>P. L. Bartlett and A. T. Stelbovics, *At. Data Nucl. Data Tables* **86**, 235 (2004).

<sup>25</sup>Actually, the multiple inelastic scattering and the cascade of lower-energy scatterings increase the calculated excitation cross section.

<sup>26</sup>K. Sagisaka, D. Fujita, and G. Kido, *Phys. Rev. Lett.* **91**, 146103 (2003).

<sup>27</sup>H. Kawai and O. Narikiyo, *J. Phys. Soc. Jpn.* **73**, 417 (2004).

<sup>28</sup>D. Farías *et al.*, *Phys. Rev. Lett.* **91**, 016103 (2003).